2nd URSI AT-RASC, Gran Canaria, 28 May – 1 June 2018

Analysis of Static Analog Linearizer Architectures for Power Amplifiers

Telmo R. Cunha(1), Pedro M. Tomé (1), and Cristiano J. Castela(1)
(1) Universidade de Aveiro – Instituto de Telecomunicações, Aveiro, Portugal, 3810-193, http://www.ua.pt

Abstract

As next generation (5G) cellular transmitters are foreseen to operate with very wide bandwidths, and with aggregates of medium-power amplifiers, the traditional use of digital predistortion (DPD) will be certainly restricted. Therefore, the incorporation of analog circuitry along with the power amplifier to compensate, in part, the generated distortion is a plausible solution to relax the complexity of the DPD algorithms. In this sense, this paper presents an analysis of possible architectures for implementing static analog linearizers for power amplifier circuits, indicating their advantages and disadvantages. The objective is to provide system level support for possible implementations of analog linearizers.

1. Introduction

User services supported on cellular networks are continuously pushing for higher bitrates, which leads wireless transceivers to require wider bandwidths. Also, power management and saving concerns are seen as critical issues, and the current spreading of electromagnetic power throughout the space surrounding the base-station is no longer an adequate solution. In this sense, base-stations for the next generation of cellular networks (5G) will most likely be composed of antenna arrays, where each antenna element is sourced by its own amplifier circuit that is on the Watt power range (and not in the hundreds of Watt range) and prepared to transmit signals within a bandwidth of several tens to hundreds of MHz.

These new requirements are challenging for the current digital predistortion (DPD) techniques, as the digital processors implementing the linearization algorithms require a sampling frequency that scales with the signal bandwidth, but also does its power consumption – leading to linearizers that would most certainly consume more power than the amplifier they are trying to compensate.

This scenario opens room for analog compensation techniques, which do not operate with sampled signals and whose bandwidth restrictions can be set through the selection of adequate electronic components and circuit elements. Naturally, it is not expected that analog linearizers would lead to identical linearization results as DPDs, as the former would hardly present the same level of configurability and degrees of freedom of the latter. Nevertheless, any improvement in the analog transmitter's linearity, if not sufficient, will decrease the complexity of the DPD algorithm, making it possible to reduce the power consumption, per amplifying path, of the digital part of the transmitter.

Analog linearization is not a new concept, and different strategies have been implemented in the past – some examples are shown in [1–5]. However, these approaches assume from the start a topology for the analog linearization architecture (such as predistortion or feed-forward) without analyzing, from a system-level perspective, how its block constitution would be for the specific case of a power amplifier (PA), nor how the transfer function shape of each constituting block would be like. This is a relevant issue since the hardware requirements for implementing a specific function (or slight variations of it) with analog components can be significantly reduced when compared to the implementation of generic functions (such as polynomials). This paper intends to contribute to this topic by providing, from a system level perspective, the block diagram definition (and the nature of each of the block functions) of possible architectures that could be implemented with analog circuitry to compensate the distortion in PAs. In addition, practical implementation comments are also provided for each analyzed architecture.

As the main contribution to the generation of distortion in PAs is attributed to their static input-output characteristics (namely, the AM-AM and AM-PM) [6], this paper analyses only the case of static analog predistortion.

2. PA Static Model Formulation

The design of the presented linearizer architectures is based on the mathematical model of the PA input-output behavior. As the PA circuit is mainly sensitive to the input signal amplitude (and not to the phase/frequency variations of the carrier signal), its behavior can be described by the AM-AM and AM-PM characteristics. Therefore, the static model considered for the PA input-output behavior, where $x(t) = b(t)\cos\big(\omega_0 t + \beta(t)\big)$ is the input modulated signal, generates the PA output, $y(t)$, according to

$$y(t) = f_a[b(t)]\cos\big(\omega_0 t + \beta(t) + f_\phi[b(t)]\big) \qquad (1).$$

In (1), the static function $f_a[\cdot]$ represents the PA's AM-AM characteristic, and $f_\phi[\cdot]$ is the PA's AM-PM static model.

3. Analog Predistorter Architecture Analysis

The analog predistorter (APD) for a certain PA circuit can be designed to directly operate over the RF modulated signal that reaches the PA input (named here as the RF-APD), or can transform the input signal still at the baseband level (denominated BB-APD), or a mixture of the two cases can be considered (the Mx-APD). Since specific electronic components are considered for each of the RF or baseband cases, it could be thought that a mixture of the two solutions would not be considered; however, as is shown, this seems to be, indeed, one of the natural possibilities which, from the topological viewpoint, leads to simple architectures.
In the following sections, possible architectures for these APD approaches are described.

3.1 Analysis of the Static RF-APD Approach

In Fig. 1 is depicted the topological architecture of a common transmitter stage to which a RF-APD was added. This APD processes the modulated signal, at the fundamental frequency $\omega_o = 2\pi f_o$, changing its amplitude and phase so that the overall transmitter is linear.

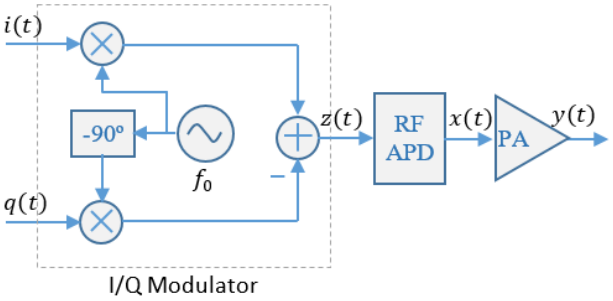

Figure 1. General transmitter with an analog predistorter operating on the RF signal (the RF-APD).

Since the RF-APD is operating directly on the RF signal at the fundamental frequency, it needs simply to independently compensate for the AM-AM and AM-PM distortions of the PA. To demonstrate this, let us consider that the RF-APD implements the following model:

$$x(t) = h_a[a(t)]\cos\big(\omega_0 t + \phi(t) + h_\phi[a(t)]\big) \qquad (2)$$

for the modulator output signal given by

$$z(t) = a(t)\cos\big(\omega_0 t + \phi(t)\big) \qquad (3).$$

Thus, the linearization conditions for the whole transmitter (in this case, the RF-APD and PA cascade) are

$$\begin{cases} f_a\big[h_a[a(t)]\big] = Ga(t) \\ \phi(t) + h_\phi[a(t)] + f_\phi\big[h_a[a(t)]\big] = \phi(t) \end{cases} \qquad (4)$$

where G is the desired gain of the linearized transmitter. The evident solution of (4) is

$$\begin{cases} h_a[a(t)] = f_a^{-1}[Ga(t)] \\ h_\phi[a(t)] = -f_\phi\big[f_a^{-1}[Ga(t)]\big] \end{cases} \qquad (5)$$

where $f_a^{-1}[\cdot]$ is the inverse function of $f_a[\cdot]$.
Topologically, the static RF-APD structure that implements the functions defined in (5) is that shown in Fig. 2. As seen in (5) and in Fig. 2, it is a system that responds to the envelope amplitude, $a(t)$, of the RF modulated signal, impacting on the envelope amplitude and phase, $b(t)$ and $\beta(t)$, respectively.

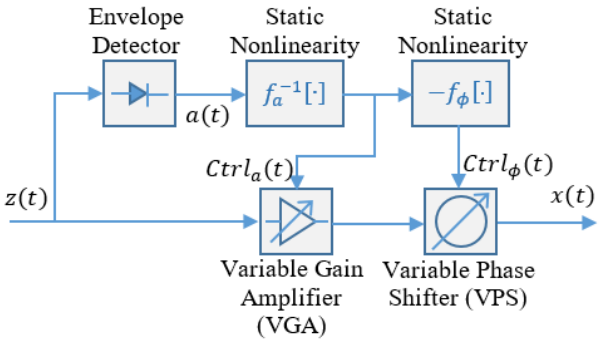

Figure 2. Topology of the static RF-APD that compensates for the PA AM-AM and AM-PM nonlinear characteristics.

The two static nonlinearity blocks in Fig. 2 operate at baseband, effectively, as the envelope detector retrieves the amplitude of the RF modulated signal – thus, the topology of Fig. 2 is, in fact, of an Mx-APD. These two blocks implement the static functions related with the PA AM-AM and AM-PM, generating the two control signals ($Ctrl_a(t)$ and $Ctrl_\phi(t)$) that set the gain and phase of the variable gain amplifier (VGA) and variable phase shifter (VPS), respectively. It must be noted, however, that the bandwidth of operation of the $f_a^{-1}[\cdot]$ static nonlinearity block must be that of the envelope amplitude, $a(t)$. As is known, the bandwidth of $a(t)$ is considerably higher than the bandwidth of the original baseband complex envelope signal. Moreover, the $-f_\phi[\cdot]$ static nonlinearity block must operate with an even higher bandwidth since its input results from the nonlinear processing of the (already wideband) $a(t)$ signal.
Another issue to consider is that common off-the-shelf VGA and VPS units allow only a very low bandwidth for their control signal, whereas in the case of Fig. 2 it would be required a very wide bandwidth at this port (although at the baseband range). Therefore, this implementation would most probably require dedicated VGA and VPS circuits.
Moreover, VGAs usually present a non-constant AM-PM characteristic, and VPSs may have non-flat AM-AM, which decreases the effectiveness of this predistorter.

3.2 Analysis of the Static BB-APD

For the case of the baseband implementation of an APD (the BB-APD), it is assumed that the baseband signals available for the BB-APD to process are the in-phase, $i(t)$, and quadrature, $q(t)$, components of the complex envelope

input signal. Later, it will also be considered the case of directly processing the amplitude, $a(t)$, and phase, $\phi(t)$, of such complex envelope signal (which, from the system level point of view, seems a more adequate choice).
In Fig. 3 is depicted the most general BB-APD block that could be considered to compensate the static PA AM-AM and AM-PM characteristics. It is, naturally, a dual-input dual-output block, which can be represented by the two real-valued two-dimensional functions in (6).

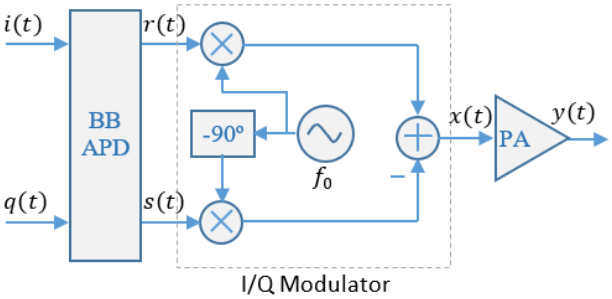

Figure 3. General transmitter with an analog predistorter operating over the baseband in-phase and quadrature signals (the Cartesian BB-APD).

$$\begin{cases} r(t) = g_I[i(t), q(t)] \\ s(t) = g_Q[i(t), q(t)] \end{cases} \tag{6}$$

According to the mixing performed by the I/Q modulator, the PA output signal, following (1), is

$$y(t) = f_a\left[\sqrt{r(t)^2 + s(t)^2}\right]\cos\left(\omega_0 t + \operatorname{atan}\left(\frac{s(t)}{r(t)}\right) + f_\phi\left[\sqrt{r(t)^2 + s(t)^2}\right]\right) \tag{7}$$

Therefore, the linearization conditions are (where the time dependency was omitted for simplicity)

$$\begin{cases} f_a\left[\sqrt{g_I[i,q]^2 + g_Q[i,q]^2}\right] = G\sqrt{i^2 + q^2} \\ \operatorname{atan}\left(\frac{g_Q[i,q]}{g_I[i,q]}\right) + f_\phi\left[\sqrt{g_I[i,q]^2 + g_Q[i,q]^2}\right] = \\ \qquad = \operatorname{atan}\left(\frac{q}{i}\right) \end{cases} \tag{8}$$

Solving (8) in order to the nonlinear static functions $g_I[\cdot]$ and $g_Q[\cdot]$ yields the (not so simple) expressions in (9) and (10), respectively, defined with respect to (11).

$$g_I[i,q] = f_a^{-1}\left[G\sqrt{i^2 + q^2}\right]\cos(\alpha) \tag{9}$$

$$g_Q[i,q] = f_a^{-1}\left[G\sqrt{i^2 + q^2}\right]\sin(\alpha) \tag{10}$$

$$\alpha = \operatorname{atan}\left(\frac{q}{i}\right) - f_\phi\left[f_a^{-1}\left[G\sqrt{i^2 + q^2}\right]\right] \tag{11}$$

Not surprisingly, expressions (9, 10) reveal the amplitude- and phase-oriented interpretation of the PA behavior, as the $i(t)$ and $q(t)$ signals appear in those equations in the form of $\sqrt{i(t)^2 + q(t)^2} = a(t)$, the original complex envelope amplitude, and of $\operatorname{atan}(q(t)/i(t)) = \phi(t)$, the phase of the input complex envelope. Naturally, this would suggest that the first block of the BB-APD would be, in fact, an element that transforms the I/Q signals into their corresponding polar form (with an increase in bandwidth).
One interesting observation that (9, 10) reveal is that the PA static nonlinearities could not be compensated if the BB-APD functions $g_I[\cdot]$ and $g_Q[\cdot]$ would be single-input functions. If those functions were just restricted to $r(t) = g_I[i(t)]$ and $s(t) = g_Q[q(t)]$, then there would not be sufficient degrees of freedom in such BB-APD to compensate for the PA static AM-AM and AM-PM behavior. This is a natural consequence of the fact that these two PA characteristics are a function of the amplitude of the input envelope.
Looking at the expressions of (9–11), the topology of a BB-APD that implements such relations can be designed, which is shown in Fig. 4.

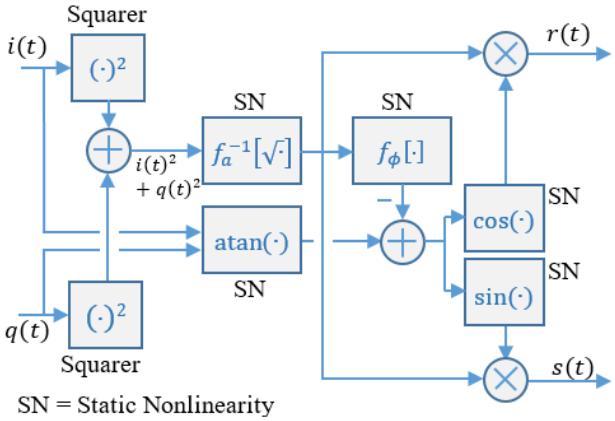

Figure 4. Topology of a static Cartesian BB-APD.

As the diagram of Fig. 4 illustrates, the implementation of the BB-APD that directly processes the in-phase and quadrature input signals is rather complex. Besides two squarers, two multipliers and adders, it requires five static nonlinear blocks, one of which being dual-input.
Notice that the input of the block that implements $f_a^{-1}[\cdot]$ receives an input whose bandwidth is twice that of the $i(t)$ and $q(t)$ signals, but that is only due to the fact that the square-root operator was accommodated into the $f_a^{-1}[\cdot]$ block (and, as before, so was the multiplication by the G gain). The signal output by the $f_a^{-1}[\cdot]$ block occupies the same bandwidth as its equivalent block of the RF-APD topology in Fig. 2.
However, contrary to the RF-APD, the BB-APD of Fig. 4 has all its elements operating at baseband, not requiring any additional RF component.
As mentioned before, the level of complexity of the topology of this BB-APD is mostly due to the conversion between the Cartesian $i(t)/q(t)$ representation into the polar representation, $a(t)/\phi(t)$. Thus, let us now consider

that the transmitter receives the amplitude and phase signals at its baseband input. Even realizing that this is not the common case, the clear complexity reduction on the BB-APD architecture encourages its analysis.

This polar BB-APD would receive as inputs the $a(t)$ and $\phi(t)$ real signals, and generate the predistorted complex envelope amplitude, $b(t)$, and phase, $\beta(t)$, signals. A modulator would then use these signals to modulate the carrier wave at frequency f_o to form the PA input signal.

Following the same approach to retrieve the linearization conditions of this transmitter, it is simple to reach the topology of this polar BB-APD, shown in Fig. 5.

With this polar-oriented approach, the modulator that would be most suited for this implementation would also be a polar modulator, instead of the traditional Cartesian I/Q modulator. Such polar modulator could be implemented through the cascade of a VGA and a VPS, whose control signals are those provided by the polar BB-APD. Figure 6 presents the overall topology of the transmitter that, using polar-oriented predistortion (again, an Mx-APD), is suited for compensating the PA AM-AM and AM-PM static characteristics.

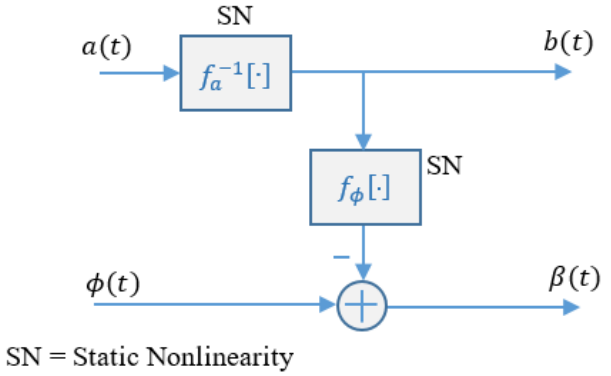

Figure 5. Topology of the static polar BB-APD.

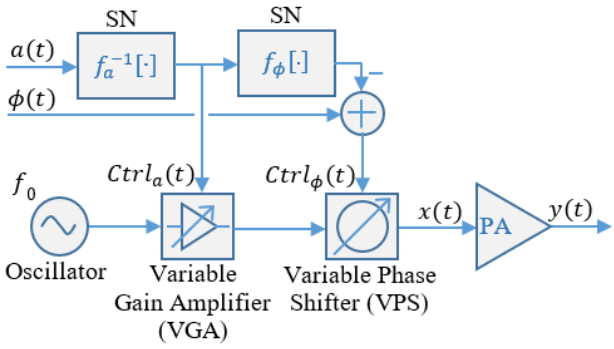

Figure 6. Overall transmitter topology with the static polar BB-APD and polar modulator.

4. Conclusions

Different topological approaches for implementing analog predistorters were presented, highlighting the frequency band of operation of their required components (either at the fundamental RF frequency or at baseband), and some of their advantages and difficulties. The point that this analysis intends to stress is that, through this system-level analysis, the topology and the nonlinear static functions to be implemented by analog circuitry are defined *a priori*, which allows designing circuits for implementing just those functions (including possible adjustment/tuning capabilities), instead of assuming circuits that aim for general function implementations (such as circuits implementing polynomials or artificial neural networks) – this should lead to much simpler circuits (with possible lower power consumption).

5. Acknowledgements

This work is funded by the National Portuguese Funds through FCT - Fundação para a Ciência e a Tecnologia under the projects UID/EEA/50008/2013 and PTDC/EEI-TEL/7049/2014 (Lin5GPA), and by the Instituto de Telecomunicações through project APIC.

6. References

1. F. Roger, "An analog approach to power amplifier predistortion," *Microwave Journal*, **54**, 4, April 2011, pp. 60-77.

2. S. Chung, J. W. Holloway, and J. L. Dawson, "Energy-efficient digital predistortion with lookup table training using analog cartesian feedback," *IEEE Transactions on Microwave Theory and Techniques*, **56**, 10, October 2008, pp. 2248-2258.

3. R. N. Braithwaite, "Analog linearization techniques suitable for RF power amplifiers used in integrated transmitters," *IEEE Proc. of Compound Semiconductor Integrated Circuit Symposium* (CSICS), **1**, 1, Monterey, CA, October 2013, pp. 1-4.

4. F. Roger, "A 200mW 100MHz-to-4GHz 11th-order complex analog memory polynomial predistorter for wireless infrastructure RF amplifiers," *IEEE Int. Solid-State Circuits Conf. Dig. of Technical Papers* (ISSCC), **1**, 1, San Francisco, CA, February 2013, pp. 94-95.

5. M. Cho, and J. S. Kenney, "Variable phase shifter design for analog predistortion power amplifier linearization system," *IEEE Wireless and Microw. Tech. Conf.* (WAMICON), **1**, 1, Orlando, FL, April 2013, pp. 1-5.

6. D. Mirri, F. Filicori, G. Iuculano, and G. Pasini, "A nonlinear dynamic model for performance analysis of large-signal amplifiers in communication systems," *IEEE Trans. Instrumentation and Meas.*, **43**, 2, April 2004, pp. 341-350.